Drug repurposing against MERS CoV and SARS-COV-2 PL^{pro} *in silico*

Abdo Elfiky (abdo@sci.cu.edu.eg)
Cairo University
Noha Ibrahim
Cairo University
Wael Elshemey
Islamic University in Madinah

Research Article

Keywords: MERS-CoV, SARS-COV-2, Papain-like protease, PLpro, Molecular Docking, Protease inhibitors

Posted Date: March 31st, 2020

DOI: https://doi.org/10.21203/rs.3.rs-19600/v1

Abstract

Aim: The Middle East Respiratory Syndrome coronavirus (MERS-CoV) and COVID-19 cause severe acute, deadly, pneumonia. Papain-like protease (PL^{pro}), is HCoV cysteine protease encoded within the Non-Structural protein 3.

Materials and Methods: Molecular docking is performed to test the binding performance of six protease inhibitors against MERS CoV and SARS-CoV-2 PL^{pro}.

Results: The compound, GRL-0667, shows the highest binding affinity to MERS CoV PL^{pro}, while Grazoprevir shows the highest binding affinity against HCV NS3. Moreover, the interaction pattern in the case of HCV NS3 is the same as in the case of coronaviruses.

Conclusion: The present study shows the ability of some anti-SARS CoV and anti-HCV NS3 drugs to inhibit MERS CoV PL^{pro}, interestingly, including the newly emerged SARS-COV-2 PL^{pro}.

Introduction

Coronaviruses (CoVs) are non-segmented, enveloped, positive-sense RNA viruses [1]. CoVs are the largest group of viruses from the *Nidovirales* order, which includes *Coronaviridae, Arteriviridae, Mesoniviridae,* and *Roniviridae* families [1, 2]. The viral particles are spherical, with diameters of approximately 125 nm. Coronavirus particles contain four main structural proteins which are the spike (S), membrane (M), envelope (E), and nucleocapsid (N) proteins, all of which are encoded within the 3' end of the viral genome (30kb) [3]. Inside the host cell, different CoV non-structural proteins (NSPs) are translated after RNA processing by viral and host-cell proteases. NSPs drive viral genome replication and subgenomic RNA synthesis [4–6].

Human Coronaviruses (HCoV) is a zoonotic disease that transmits from animals to humans [7–9]. There are seven strains of HCoV: 229E, NL63, OC43, HKU1, Severe Acute Respiratory Syndrome (SARS), Middle-East Respiratory Syndrome (MERS), and the newly emerged SARS-COV–2 [4, 7, 10–15]. The seven HCoV strains are classified into alpha (229E and NL63) and beta coronaviruses (OC43, HKU1, SARS, MERS, and SARS-COV–2) [16, 17].

HCoV encodes either two or three proteases that cleave the viral polyprotein; cysteine protease, a serine protease, and the main protease (Mpro) which are encoded by NSPs. Most coronaviruses encode two Papain-like proteases (PL^{pro}) proteins within NSP3, except the γ-coronaviruses [16, 18]. On the other hand, SARS-CoV and MERS-CoV only express one PL^{pro}. The MERS-CoV encodes many types of proteins such as the Mpro, which includes the chymotrypsin-like protease (3CL protease), and the PL^{pro} [18]. The first three positions between non-structural proteins are cleaved by PL^{pro}, while the other eleven positions are cleaved by $3CL^{pro}$ [18].

PL^{pro} is a multifunctional cysteine protease that processes the viral polyprotein and hosts cell proteins by hydrolyzing the peptide and isopeptide bonds in viral and cellular substrates leading to viral replication [18]. This is required for the cleavage of the polyprotein into its 16 viral proteins that involved in the formation of a membrane-associated cytoplasmic enzyme complex (the replicase complex), which is responsible for directing the replication and transcription of the viral genome [4, 18]. PL^{pro} is recognized to be involved in deubiquitination, de-ISGylation, and viral evasion of the innate immune response [18]. Despite the presence of several solved structures for SARS and MERS PL^{pro}, no solved structure is available (at the time of writing this manuscript) for the SARS-COV–2 PL^{pro}.

Most of the drugs that inhibit SARS and MERS-CoV targets are encoded in the 50-terminal two-thirds of the genome, within the two open reading frames (ORF1a and ORF1ab) that encode for the NSPs. Telaprevir and Boceprevir have approved inhibitors against Hepatitis C Virus (HCV) in the year 2011 by the US Food and Drugs Administration (FDA), while Grazoprevir was approved by FDA in 2016, against HCV as well [19–22]. Grazoprevir is a direct-acting antiviral drug used as part of combination therapy to HCV. It is an inhibitor of NS3/4A, a serine protease, encoded by HCV genotypes 1 and 4 [19]. Additionally, Telaprevir and Boceprevir belong to the class of organic compounds known as hybrid peptides. [19, 23–25]. On the other hand, mycophenolic acid is an antibiotic compound derived from *Penicillium stoloniferum.* It blocks the *de novo* biosynthesis of purine nucleotides as it inhibits the enzyme inosine monophosphate dehydrogenase [26]. Mycophenolic acid, in addition to the two dioxolane derivatives (GRL–0667 and GRL–0617), inhibits the SARS PL^{pro} [27].

Materials And Methods

MERS CoV PL^{pro} sequences (FASTA) and coordinates (PDB) are downloaded from the Protein Data Bank database [28]. The PDB IDs of the downloaded MERS CoV PL^{pro} are (4RNA, 5KO3, 4RF1, 5V69, 4PT5, 4REZ, 4RF0, 4R3D, 6BI8 and 4WUR). The resolution of the structures ranges from 1.79Å to 3.16Å, and the structures are solved during the last five years. Multiple Sequence Alignment (MSA) is carried out for the downloaded sequences using the T-Coffee web server [29]. The MSA is represented by the ESpript 3.0 web server, which provides enhanced graphical information for the aligned sequences [30]. By the aid of PyMOL software [31], PL^{pro} structures are prepared for the docking step. This includes removing water molecules, ions, and ligands. Additionally, polar Hydrogens are added, and the processed structures are saved in the PDB format for the docking study. Zn^{+2} ions are retained in the structures due to its crucial role in protein function [32–34].

AutoDock vina [35] is used in this study to perform molecular docking of N-(1,3-benzodioxol–5-ylmethyl)–1-[(1R)–1-naphthalen–1-ylethyl]piperidine–4-carboxamide (GRL–0667), 5-amino–2-methyl-N-[(1R)–1-naphthalen–1-ylethyl]benzamide (GRL–0617), Telaprevir, Mycophenolic acid, and Boceprevir to MERS PL^{pro} active site (C111, H278, and D293). The 3D structures of the inhibitors are retrieved from the Protein Data Bank with the following PDB IDs: 3MJ5 (GRL–0667 complexed with SARS NS3 protease), 3E9S (GRL–0617 complexed with SARS NS3 protease), 3SV6 (Telaprevir complexed with HCV NS3/4A

protease), 1JR1 (Mycophenolic acid complexed with Cricetulus *griseus* Inosine Monophosphate Dehydrogenase) and 3LOX (Boceprevir complexed with HCV NS3/4A protease) and Grazoprevir. AutoDock Vina is used with the flexible active site / flexible ligand protocol [35, 36]. MERS PL^{pro} active site (C111, H278, and D293) is treated as flexible during the docking experiments. Protein-Ligand Interaction Profiler (PLIP) web server is utilized to analyze the docking complexes [37]. Four types of interactions are established upon docking: H-bonding, hydrophobic interactions, salt bridges, and π-stacking. The average docking scores and the residues that take part in the interactions are analyzed.

Results

Figure 1A shows the multiple sequence alignment (MSA) of the available solved structures of MERS CoV PL^{pro} (PDB IDs: 4RNA, 5KO3, 4RF1, 5V69, 4PT5, 4REZ, 4RF0, 4R3D, 6BI8, and 4WUR). The conserved domains are highlighted in red. The black rectangles mark active site residues (C111, H278, and D293) dashed columns. The secondary structure is found at the top of the MSA for one of the structures (PDB ID: 4R3D), while the surface accessibility is at the bottom of the MSA with the default coloring scheme. On the other hand, figures 1B and 1C show the pairwise sequence alignment between MERS CoV PL^{pro} (PDB ID: 4RNA) against both SARS CoV PL^{pro} (PDB ID: 5Y3Q), and HCV NS3/4A protease (PDB ID: 6DIQ), respectively. Secondary structures and surface accessibilities are shown in the top and bottom of the alignments, respectively. Active site residues for MERS CoV PL^{pro} (C111, H278, and D293), and SARS CoV PL^{pro} (C112, H273, and D287) are marked by black-dashed columns, while for HCV NS3/4A protease the active residues (H1057, D1081, and S1139) are marked by the orange dashed columns.

Figure 2 shows the docking scores calculated using AutoDock Vina software for the docking of the six compounds into MERS CoV PL^{pro}, SARS CoV PL^{pro}, and HCV NS3 protease active sites. MERS CoV is represented in blue diamonds with error bars representing the standard deviation (SD). Red and green lines represent SARS CoV PLpro and HCV NS3 proteases, respectively. The compound GRL–0667 shows the best result for docking into PL^{pro} of the SARS-COV–2 model (green circle).

Table 1 shows the amino acids involved in the interactions with GRL–0667 for MERS PL^{pro}, SARS PL^{pro}, SARS-COV–2 $PL^{pro,}$ and HCV NS3. Each interacting residue is listed with the number of formed interactions. The interactions involve Hydrophobic, H-bonding, salt bridges and π-π stacking.

Table 1 The interactions formed between GRL-0667 and MERS PL^{pro}, SARS PL^{pro}, SARS-CoV-2 PL^{pro}, and HCV NS3 upon docking. The Star (*) represents salt bridges while the douple stars (**) represent π-π contact.

Protein	*PDB ID*	*Docking score (kcal/mol)*	*H-bonding*		*Hydrophobic interaction*	
			number	Residues involved	number	Residues involved
MERS PL^{pro}	4PT5	-6.7	3	**D293***, Y407 (2)	5	**V338**, T377, **F397**, **V404** (2)
	4R3D	-7.1	1	**D293***	3	R296, **V338**, **F397**
	4REZ	-7.3	2	**D293***, **D293**	6	P291, **F397****, **F397** (3), Y407
	4RF0	-8.3	1	**D293**	6	P291, T377, **F397** (2), **V404** (2)
	4RF1	-8.1	1	**D293***	7	**D293**, R296 (2), **V338**, T377, **F397** (2)
	4RNA	-8.2	2	**D293***, Y407	8	**D293**, R296 (2), **V338** (2), T377, **F397**, **V404**
	4WUR	-8.6	2	**D293***, Y407	7	R314 (2), **V338**, **F397** (2), Y407
	4KO3	-7.4	2	**D293***, R296	5	**D293**, R296, L297 (2), **V404**
	5V69	-6.5	4	K419, D421, T424, W431	4	V396, Q398, D421, T424
	6BI8	-8.0	1	**D293**	6	P291 (2), **D293**, **F397**, **V404** (2)
SARS PL^{pro}	5Y3K	-9.3	6	W233, C238, G290, **D293***, G398, Y400	5	Y239, L289, Y391, Y400 (2)
HCV NS3	6DIQ	-8.7	3	H75, K154, S157	3	Q59, T60, F61
SARS-CoV-2 PL^{pro}	model	-7.0	3	W93, K105, W106	7	K92, W106** (3) W106 (2), A107

Discussion

MERS CoV PL^{pro} is a multifunctional cysteine protease that processes both viral polyprotein and some host-cell proteins by hydrolyzing the peptide and isopeptide bonds in the substrates [38]. In order to perform this function, a conserved active site triad is required [20, 23, 39, 40]. C111, H278, and D293 are reported to be the active site triad residues in MERS CoV PL^{pro} [1, 2]. As shown in figure 1A, the active site residues are water accessible for all solved structures of MERS CoV PL^{pro} (cyan colored boxes under the residues H278, and D293). Additionally, the active site residues C112, H273, and D287 in SARS CoV PL^{pro} (PDB ID: 5Y3Q (see figure 1B)) and H1057, and D1081 in HCV NS3/4A protease (PDB ID: 6DIQ (see figure 1C)) are water accessible (either blue or cyan boxes under the mentioned residues, where the relative accessibility is < 0.1). Exceptions are the C111 in MERS CoV PL^{pro} and S1139 in HCV NS3/4A protease where the relative accessibility is less than 0.1 (white boxes below the pairwise alignment of figures 1A, and 1C).

In this study, we used six potent anti-proteases tested earlier against Hepatitis C Virus and SARS CoV (see figure 2). GRL–0667, GRL–0617, and mycophenolic acid are anti-SARS CoV PL^{pro} inhibitors currently under clinical trials, while Grazoprevir, Telaprevir, and Boceprevir are anti-HCV NS3 protease drugs approved by the FDA. Figure 2 shows the docking score values calculated by AutoDock Vina software for the docking of GRL–0667, GRL–0617, Telaprevir, mycophenolic acid, Boceprevir, and Grazoprevir into the active site triads of the available ten MERS CoV PL^{pro} structures, one of the SARS CoV PL^{pro} structures and one HCV NS3 protease structure. All compounds are succeeded in fitting in the protease active site with binding energies ranging between –6.3 up to –9.3 kcal/mol (good binding energy). GRL–0667, GRL–0617, and mycophenolic acid have slightly better binding energies to both SARS CoV PL^{pro} (red line) and HCV NS3 protease (green line) compared to the MESR CoV PL^{pro} (blue diamonds). On the other hand, Telaprevir, Boceprevir, and Grazoprevir have better binding energies to HCV NS3 protease compared to the HCoVs (MERS and SARS); still, the difference is not significant (about 1 kcal/mol).

Our results are in support of the experimental IC50 values for each compound (see figure 2 B). Grazoprevir has the best IC50 value against HCV (4–7 pM) [19, 26], while Telaprevir and Boceprevir have slightly higher values against HCV (50 and 80 pM) [22, 40]. GRL–0667, GRL–0617, and Mycophenolic acid have IC50 values against SARS HCoV in the range of hundreds of picomolar [27].

In an attempt to test the drugs against the newly emerged Wuhan coronavirus (SARS-COV–2), we built a model for SARS-COV–2 PL^{pro} then tested the compounds. The best (based on the binding energy) compound is found to be GRL–0667 with a binding energy of –7 kcal/mol. This value is in the same range of that for MERS HCoV PL^{pro} (–7.62 ± 0.65 kcal/mol) and slightly less than that of SARS HCoV PL^{pro} (–9.3 kcal/mol). Table 1 shows the detailed interaction patterns of GRL–0667 with all PL^{pro} of the coronaviruses under the study and HCV NS3. For MERS PL^{pro}, as indicated in Table 1, some residues form H-bonds, salt bridges, and hydrophobic contacts with GRL–0667 in most docking trials (in bold) including; D293 (9 out of 10 trials), V338 (5 out of 10 trials), F397 (8 out of 10 trials), and V404 (5 out of 10 trials). Additionally, P291, R296, T377, and Y407 also contribute (at least 3 out of 10 trials) in the interaction formed between GRL–0677 and MERS PL^{pro}. The active site residue D293 is involved in the

interactions between GRL–0667 and SARS PL^{pro}. As we can see from table 1, the main driving force for binding in case of MERS and SARS PL^{pro} is the H-bonds formed between GRL–0667 and D293 and at least three hydrophobic contacts around the active residue D287 (P291, R296, V338, T377, F397, V404, and Y407 in MERS PL^{pro}, and Y239, L289, Y391, and Y400 in SARS PL^{pro}). For SARS-COV–2, the main residues that take part in the interaction with GRL–0667 are the residues around the active site C111 which are surface exposed like K105, W106, and A107. Figure 3 summarizes the interaction patterns of GRL–0667 against SARS-COV–2 PL^{pro}, MERS HCoV PL^{pro}, SARS HCoV PL^{pro}, and HCV NS3 protease.

From the calculated binding energies, one can conclude that all the tested compounds can bind to the PL^{pro} of SARS, MERS, and the SARS-COV–2 strains of coronaviruses with binding energies that depend on the strain. Further modifications of these lead compounds can give more potent inhibitors that can tightly bound to the active site of PL^{pro} of the newly emerging coronaviruses.

Conclusion

Coronaviruses are repeatedly emerging viruses that infect both animals and humans. The urgent need for an effective inhibitor of crucial viral proteins is the reason for the development of new testing techniques and protocols. In this study, drug repurposing is performed to test anti-HCV and anti-SARS drugs against the Papain-like proteases of MERS CoV and SARS-COV–2. Results suggest a possible inhibitory effect of the tested drugs against the newly emerged coronaviruses. Besides, these compounds can be optimized to get more competent and potent new compounds specific against different emerging coronaviruses.

Declarations

Competing Interest

All authors declare that there is no competing interest in this work.

Data Availability

The docking structures are available upon request from the corresponding author

References

1.Zumla AC, J. F. Azhar, E. I. Hui, D. S. Yuen, K. Y.. Coronaviruses - drug discovery and therapeutic options. *Nat Rev Drug Discov* doi:10.1038/nrd.2015.37 (2016).

2.Coleman CM, Frieman MB. Coronaviruses: important emerging human pathogens. *J Virol* 88(10), 5209–5212 (2014).

3.Belouzard S, Millet JK, Licitra BN, Whittaker GR. Mechanisms of coronavirus cell entry mediated by the viral spike protein. *Viruses* 4(6), 1011–1033 (2012).

4.Qinfen Z, Jinming C, Xiaojun H *et al.* The life cycle of SARS coronavirus in Vero E6 cells*. J Med Virol* 73(3), 332–337 (2004).

5.Graham RL, Donaldson EF, Baric RS. A decade after SARS: strategies for controlling emerging coronaviruses*. Nat Rev Microbiol* 11(12), 836–848 (2013).

6.Bailey-Elkin BA, Knaap RC, Johnson GG *et al.* Crystal structure of the Middle East respiratory syndrome coronavirus (MERS-CoV) papain-like protease bound to ubiquitin facilitates targeted disruption of deubiquitinating activity to demonstrate its role in innate immune suppression*. Journal of Biological Chemistry* 289(50), 34667–34682 (2014).

7.Azhar EI, El-Kafrawy SA, Farraj SA *et al.* Evidence for camel-to-human transmission of MERS coronavirus*. N Engl J Med* 370(26), 2499–2505 (2014).

8.Corman VM, Baldwin HJ, Tateno AF *et al.* Evidence for an ancestral association of human coronavirus 229E with bats*. Journal of virology* JVI. 01755–01715 (2015).

9.Han HJ, Yu H, Yu XJ. Evidence for zoonotic origins of Middle East respiratory syndrome coronavirus*. The Journal of general virology* 97(2), 274–280 (2016).

10.Zumla A, Hui DS, Perlman S. Middle East respiratory syndrome*. The Lancet* 386(9997), 995–1007 (2015).

11.Stadler K, Masignani V, Eickmann M *et al.* SARS—beginning to understand a new virus*. Nat Rev Microbiol* 1(3), 209–218 (2003).

12.Yang L. China confirms human-to-human transmission of coronavirus*.* (2020).

13.Hui DS, I Azhar E, Madani TA *et al.* The continuing 2019-nCoV epidemic threat of novel coronaviruses to global health — The latest 2019 novel coronavirus outbreak in Wuhan, China*. International Journal of Infectious Diseases* 91 264–266 (2020).

14.Huynh J, Li S, Yount B *et al.* Evidence supporting a zoonotic origin of human coronavirus strain NL63*. Journal of virology* 86(23), 12816–12825 (2012).

15.Elfiky AaI, N. S. Anti-SARS and anti-HCV drugs repurposing against the Papain-like protease of the newly emerged coronavirus (2019-nCoV)*. preprint* doi:10.21203/rs.2.23280/v1 (2020).

16.Sharif-Yakan A, Kanj SS. Emergence of MERS-CoV in the Middle East: origins, transmission, treatment, and perspectives*. PLoS Pathog* 10(12), e1004457 (2014).

17.Elfiky AA, Mahdy SM, Elshemey WM. Quantitative structure-activity relationship and molecular docking revealed a potency of anti-hepatitis C virus drugs against human corona viruses*. Journal of Medical Virology* 89(6), 1040–1047 (2017).

18.Báez-Santos YM, John SES, Mesecar AD. The SARS-coronavirus papain-like protease: structure, function and inhibition by designed antiviral compounds. *Antiviral research* 115 21–38 (2015).

19.Gonzalez-Grande R, Jimenez-Perez M, Gonzalez Arjona C, Mostazo Torres J. New approaches in the treatment of hepatitis C. *World J Gastroenterol* 22(4), 1421–1432 (2016).

20.Saleh NA, Elfiky AA, Ezat AA, Elshemey WM, Ibrahim M. The Electronic and Quantitative Structure Activity Relationship Properties of Modified Telaprevir Compounds as HCV NS3 Protease Inhibitors. *Journal of Computational and Theoretical Nanoscience* 11(2), 544–548 (2014).

21.Tong J, Wang YW, Lu YA. New developments in small molecular compounds for anti-hepatitis C virus (HCV) therapy. *J Zhejiang Univ Sci B* 13(1), 56–82 (2012).

22.Sarrazin C, Hézode C, Zeuzem S, Pawlotsky J-M. Antiviral strategies in hepatitis C virus infection. *Journal of Hepatology* 56 S88-S100 (2012).

23.Ezat AA, Elfiky AA, Elshemey WM, Saleh NA. Novel inhibitors against wild-type and mutated HCV NS3 serine protease: an in silico study. *VirusDisease* doi:10.1007/s13337–019–00516–7 (2019).

24.Nagpal N, Goyal S, Wahi D *et al.* Molecular principles behind Boceprevir resistance due to mutations in hepatitis C NS3/4A protease. *Gene* 570(1), 115–121 (2015).

25.Chase R, Skelton A, Xia E *et al.* A novel HCV NS3 protease mutation selected by combination treatment of the protease inhibitor boceprevir and NS5B polymerase inhibitors. *Antiviral research* 84(2), 178–184 (2009).

26.Dore GJ, Altice F, Litwin AH *et al.* Elbasvir–grazoprevir to treat hepatitis C virus infection in persons receiving opioid agonist therapy: a randomized trial. *Annals of internal medicine* 165(9), 625–634 (2016).

27.Lee H, Lei H, Santarsiero BD *et al.* Inhibitor recognition specificity of MERS-CoV papain-like protease may differ from that of SARS-CoV. *ACS chemical biology* 10(6), 1456–1465 (2015).

28.Berman H, Henrick K, Nakamura H. Announcing the worldwide Protein Data Bank. *Nat Struct Mol Biol* 10(12), 980–980 (2003).

29.Sievers F, Wilm A, Dineen D *et al.* Fast, scalable generation of high-quality protein multiple sequence alignments using Clustal Omega. *Molecular systems biology* 7(1), 539 (2011).

30.Robert X, Gouet P. Deciphering key features in protein structures with the new ENDscript server. *Nucleic Acids Research* 42(W1), W320-W324 (2014).

31.The PyMOL Molecular Graphics System, Version 1.7.6 Schrödinger, LLC.

32.Elfiky AA, Elshemey WM. Molecular dynamics simulation revealed binding of nucleotide inhibitors to ZIKV polymerase over 444 nanoseconds. *Journal of Medical Virology* 90(1), 13–18 (2018).

33.Elfiky AA, Ismail AM. Molecular Modeling and Docking revealed superiority of IDX–184 as HCV polymerase Inhibitor. *Future Virology* 12(7), 339–347 (2017).

34.Doublie S, Ellenberger T. The mechanism of action of T7 DNA polymerase. *Curr Opin Struct Biol* 8(6), 704–712 (1998).

35.Trott O, Olson AJ. AutoDock Vina: Improving the speed and accuracy of docking with a new scoring function, efficient optimization, and multithreading. *Journal of Computational Chemistry* 31(2), 455–461 (2010).

36.Morris GM, Huey R, Lindstrom W *et al.* AutoDock4 and AutoDockTools4: Automated Docking with Selective Receptor Flexibility. *Journal of computational chemistry* 30(16), 2785–2791 (2009).

37.Salentin S, Schreiber S, Haupt VJ, Adasme MF, Schroeder M. PLIP: fully automated protein–ligand interaction profiler. *Nucleic acids research* 43(W1), W443-W447 (2015).

38.Báez-Santos YM, Mielech AM, Deng X, Baker S, Mesecar AD. Catalytic Function and Substrate Specificity of the Papain-Like Protease Domain of nsp3 from the Middle East Respiratory Syndrome Coronavirus. *Journal of Virology* 88(21), 12511–12527 (2014).

39.Saleh NA, Ezat AA, Elfiky AA, Elshemey WM, Ibrahim M. Theoretical Study on Modified Boceprevir Compounds as NS3 Protease Inhibitors. *Journal of Computational and Theoretical Nanoscience* 12(3), 371–375 (2015).

40.Ezat AA, Elshemey WM. A comparative study of the efficiency of HCV NS3/4A protease drugs against different HCV genotypes using in silico approaches. *Life Sciences* 217 176–184 (2019).

Figures

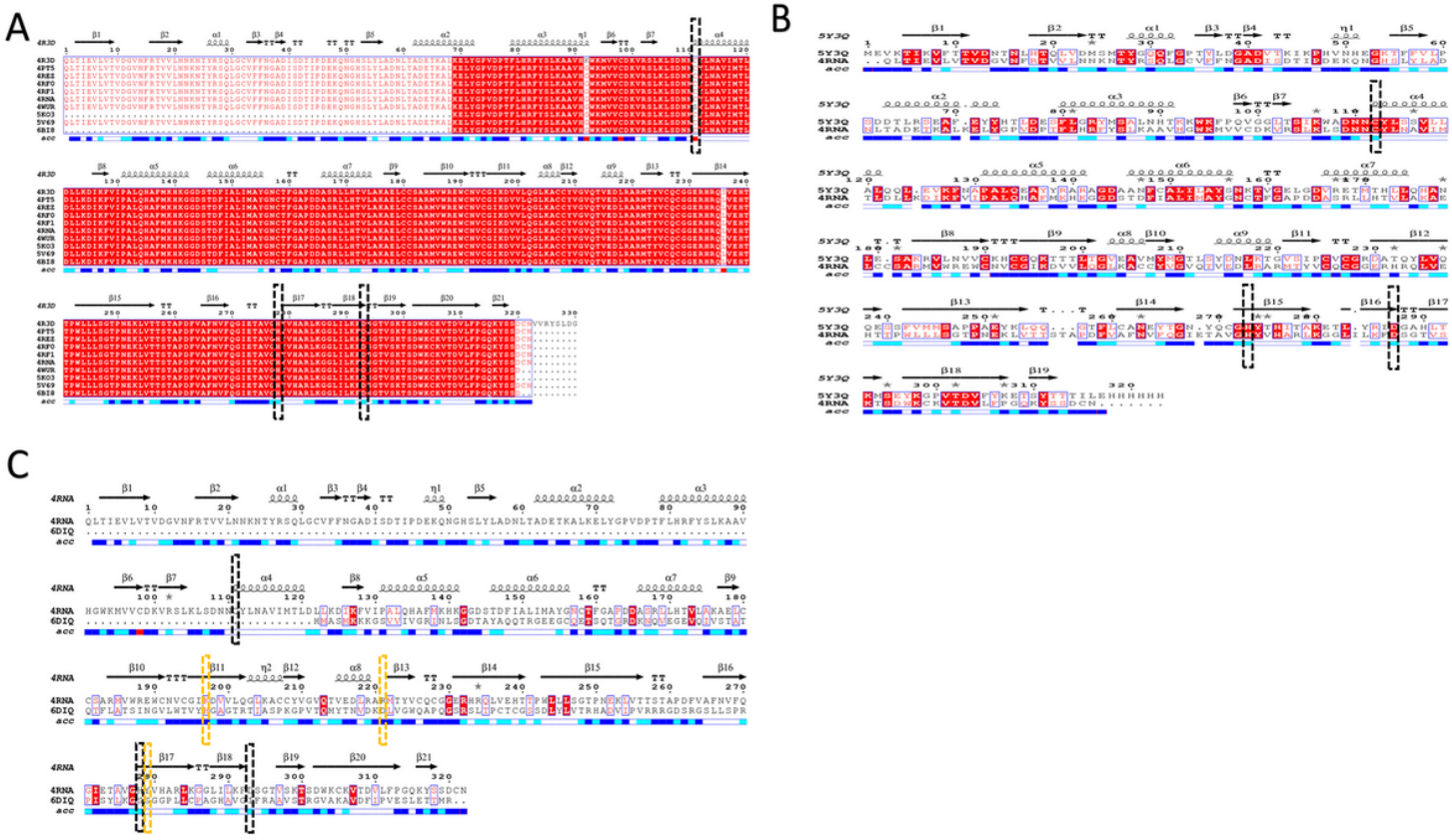

Figure 1

(A) Multiple sequence alignment of the ten available MERS CoV PLpro in the protein data bank. Identical residues are highlighted in red while highly conserved in yellow. Secondary structures are shown at the top of the MSA for the structure (4R3D). Surface accessibility is shown at the bottom of the MSA with blue for highly accessible, cyan partially accessible, and white for buried residues. Black-dashed rectangles mark the active site triad (C111, H278, and D293). On the other hand, the pairwise sequence alignment between MERS PLpro and SARS PLpro (B) and HCV NS3 (C). Active site residues for MERS PLpro and SARS PLpro are both marked by black-dashed rectangles, while orange-dashed rectangles mark HCV NS3 active site.

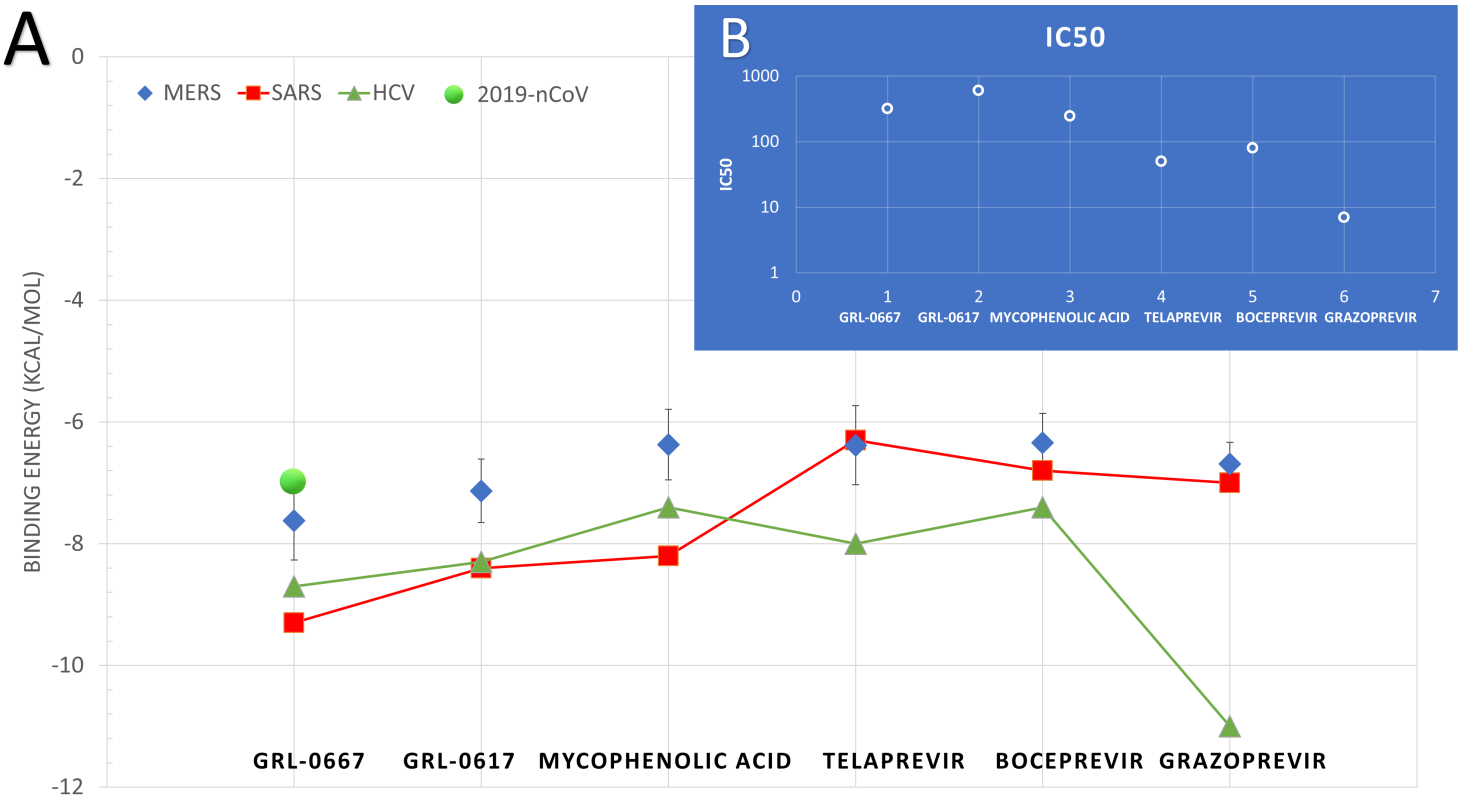

Figure 2

(A) The binding energies of; GRL-0667, GRL-0617, Telaprevir, mycophenolic acid, Boceprevir, and Grazoprevir, into the active site of HCV NS3 (green line), SARS PLpro (red line) and MERS PLpro (blue diamonds) calculated by AutoDock Vina software. For MERS PLpro, the average values are represented with the blue diamonds, while the error bars represent the standard deviation. The green circle represents the binding energy of GRL-0667 to the SARS-COV-2 PLpro model of coronavirus. (B) The Experimental IC50 values as reported from literature for the compounds under the study.

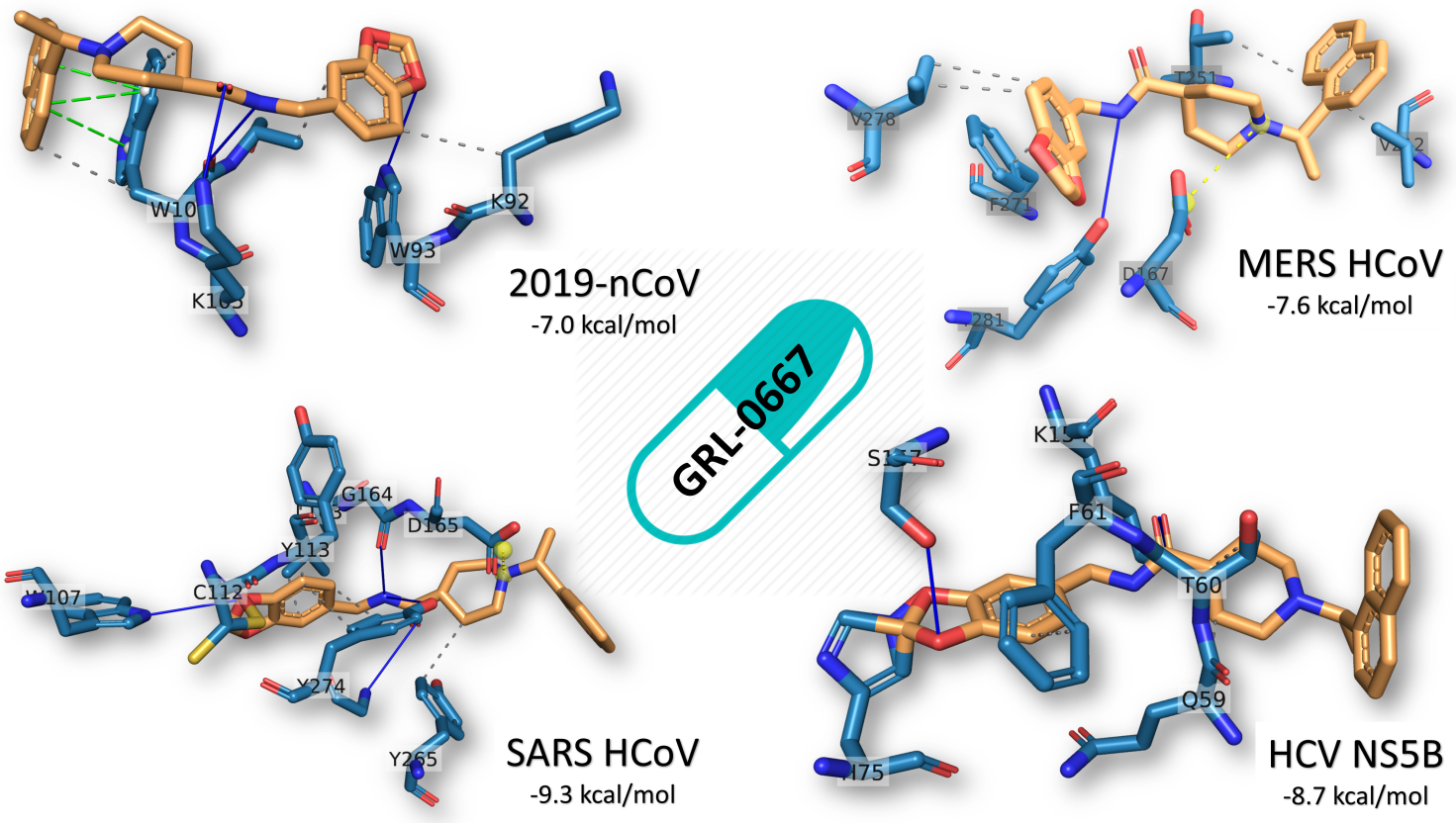

Figure 3

The interaction patterns of the docked GRL-0667 (orange sticks) to SARS-COV-2 PLpro, MERS HCoV PLpro, SARS HCoV PLpro, and HCV NS3 protease (cyan sticks). Residues are labeled with its one-letter codes. H-bonds in solid blue lines while hydrophobic interactions are in dashed lines. Additionally, salt bridges and π-π stacking are represented in yellow spheres connected by dashed lines and green lines, respectively. Docking scores are listed under each complex in kcal/mol.